

RESEARCH ARTICLE

Influence of electrical polarization on thrombogenicity of titania nanotubes

Jyorthana Rajappa Muralidhar^{1,2} | Kabilan Sakthivel^{1,2} |
Madanagurusamy Sridharan² | Masanori Kikuchi¹ 

¹Bioceramics Group, National Institute for Materials Science, Tsukuba, Japan

²Centre for Nanotechnology & Advanced Biomaterials and SEEE, SASTRA University, Thanjavur, India

Correspondence

Masanori Kikuchi, Bioceramics Group, National Institute for Materials Science, 1-1, Namiki, Tsukuba, Ibaraki, 305-0044, Japan.

Email: KIKUCHI.Masanori@nims.go.jp

Abstract

The development of hemocompatible biomaterials with antithrombogenic surface coatings remains a challenge in cardiovascular applications. There is interest in negatively charged surfaces that inhibit thrombus formation through electrostatic repulsion between the biomaterial surface and negatively charged platelets. Hence, the present study investigated the influence of electrical polarization on the thrombogenicity of titania nanotubes (TNT), which are promising candidates for inhibiting thrombogenicity via surface modification. TNTs were formed on commercially pure titanium plate by the electrochemical anodization technique using platinum as a counter electrode at 60 V for 24 h with two kinds of electrolytes (hydrofluoric acid diluted with dimethyl sulfoxide [D-TNT] or ethylene glycol [E-TNT]) followed by an annealing at 540°C for 3 h in air. Both TNTs were mixture of anatase and rutile, and the D-TNT had a diameter of 108.76 ± 2.55 nm and the E-TNT, 53.833 ± 2.42 nm. The TNTs were electrically polarized at 100 V of DC field and 400°C for 1 h. Water contact angle measurements showed that the non-polarized (0-) TNT surface was hydrophilic whereas the positively (P-) or negatively (N-) polarized TNT surfaces showed high-hydrophilicity. Antithrombogenicity was evaluated using the thrombus coverage area ratio (TCAR) after soaking the TNTs in bovine whole blood. The TCARs for 0-polarized E- and D-TNTs were $5.30 \pm 4.34\%$ and $36.3 \pm 5.8\%$ and for P-polarized E-TNT and D-TNT were $1.50 \pm 0.77\%$ and $2.76 \pm 1.07\%$, whereas no thrombus formation ($0 \pm 0\%$) for N-polarized E-TNT and very few thrombus formation ($0.12 \pm 0.22\%$) for N-polarized D-TNT. The electrostatic repulsion between the N-polarized E-TNTs and platelets completely inhibits thrombus formation, which cannot be achieved by the nanomorphology and high-hydrophilicity of other TNTs. Hence, N-TNTs formed by electrical polarization are potential candidates for cardiovascular devices, such as artificial heart valves with long-term hemocompatibility.

This is an open access article under the terms of the [Creative Commons Attribution](https://creativecommons.org/licenses/by/4.0/) License, which permits use, distribution and reproduction in any medium, provided the original work is properly cited.

© 2024 The Authors. *International Journal of Ceramic Engineering & Science* published by Wiley Periodicals LLC. on behalf of the American Ceramic Society.

KEYWORDS

biocompatibility, nanotubes, polarization, surface modification, titanium dioxide

1 | INTRODUCTION

An initially adsorbed protein layer on the blood-contact biomaterial surface mainly triggers adverse reactions, such as the activation of coagulation via the intrinsic pathway, activation of leukocytes, which results in inflammation, and adhesion and activation of platelets.¹ Consequently, the number of blood cells can decrease, and a thrombus can be formed.² To overcome this drawback, blood-thinning medications are often prescribed to patients who use blood-contact devices. Antiplatelet drugs or anticoagulants were administered to reduce thrombogenicity. Such therapies can increase the risk of heart failure and internal bleeding.³ Pre-clotting the implant surface by exposing it to the patient's blood prior to implantation is another way to inhibit thrombogenicity. However, this method is only applicable to porous implants, such as vascular grafts, and is not suitable for valves and catheters.⁴

The surface of blood-contact biomaterials has been modified by synthetic and natural materials; for instance, heparin is used as a coating for stents and catheters^{5–7} and pyrolytic carbon is used as a coating for artificial heart bulbs. However, these strategies are insufficient for achieving long-term hemocompatibility.⁸ Therefore, the development of material surfaces with long-term hemocompatibility remains a significant challenge.

Titanium (Ti) and its alloys have been of great interest because of their excellent biocompatibility owing to the formation of a stable oxide layer (passive film) on their surface,^{9,10} however, the passive films on Ti and its alloys are not sufficient for intravascular use. Tubular nanotopographical cues of Ti metal, titania nanotubes (TNT), were reported to provide a better interface between the Ti and the surrounding tissues. Previous studies have shown enhanced hemocompatibility of these TNT arrays.^{11–13} Increase in the production of endothelial cell extracellular matrices on TNT was also reported.^{14–16} TNTs have been widely used for cardiovascular stent because of its prevention of platelet and smooth muscle cell adhesion and activation on to stent surfaces and support the growth of human coronary artery endothelial cells.¹⁷ However, a thrombogenicity evaluation of TNT revealed presence of some risks of forming thrombosis on the surface of the TNT.¹³ Some of the factors that influence the material's biocompatibility are their sur-

face roughness,¹⁸ surface chemistry,¹⁹ surface energy (hydrophobicity/hydrophilicity),²⁰ crystallinity,²¹ and concentration.²² The current approaches mainly focus on surface modifications with biological anticoagulants such as heparin, or anti-fouling molecules like tanfloc/heparin polyelectrolyte multilayers on TNT array surfaces.²³ Superhemophobic TNT surfaces were developed by modifying the TNT with alkyl and fluorinated silanes using a chemical vapor deposition technique.²⁴ Superhemophobic TNT was also investigated for blood-contacting devices as it can decrease surface protein adsorption/factor XII activation and delay thrombogenesis.²⁵ Thus, Ti coated with TNTs is a promising candidate to inhibit thrombogenicity but it still requires further modification to enhance antithrombogenicity.

Saito et al. reported that the negatively charged surface of a biomaterial has the potential to inhibit thrombogenesis by the electrostatic prevention of platelet adsorption on the material surface.²⁶ This suggests that the permanently negatively charged TNT surface enhances the inhibition of thrombus formation by electrostatic repulsion between the Ti surface and negatively charged platelets, in addition to its high-hydrophilicity and nanostructure. To the best of our knowledge, no previous study has reported the development of negatively charged TNTs using electrical polarization for hemocompatibility. In this study, negatively charged TNTs were developed by electrical polarization, and their influence on antithrombogenicity was investigated by evaluating thrombus formation on the surface of TNTs using anti-coagulated bovine whole blood with the activation of blood coagulation by the addition of calcium chloride (CaCl₂).

2 | MATERIALS AND METHODS

2.1 | Materials

Ti sheets (>99.5%, 0.5 mm in thickness) and platinum (Pt) foil (99.99% purity) were purchased from Nilaco Co. Formaldehyde, hydrofluoric acid (HF, 48%), ethylene glycol (EG, C₂H₆O₂, 99%), and dimethyl sulfoxide (DMSO, [CH₃]₂SO, 99.7%) were purchased from Wako Pure Chemicals, Inc. Calcium (Ca) and magnesium(Mg)-free phosphate-buffered saline was purchased from Dulbecco's PBS (DS Pharma Biomedical). Six-well tissue culture plates were purchased from Falcon. Anti-coagulated

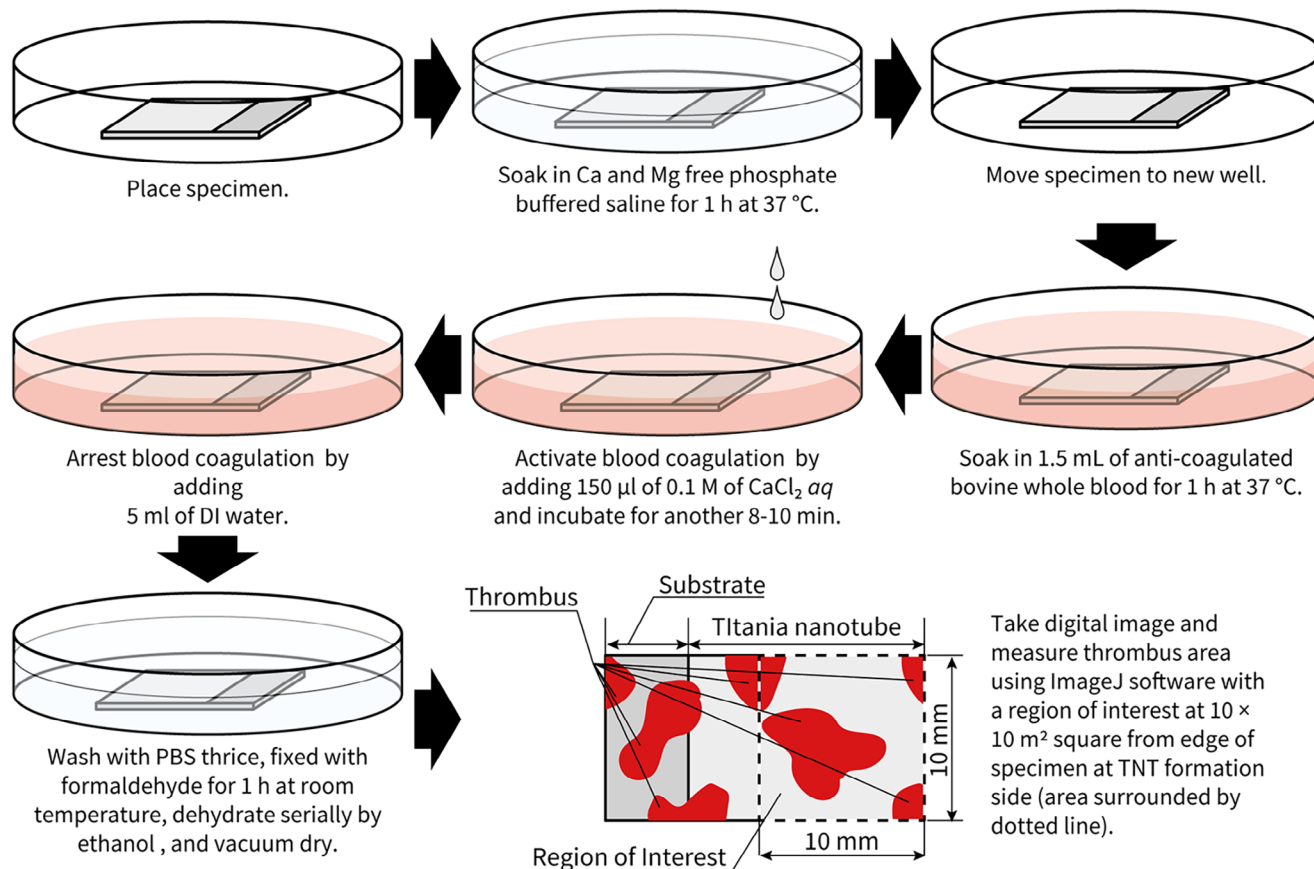


FIGURE 1 Flow of antithrombogenicity study.

bovine whole blood (cat. no. 12070610, lot. no. 7097062) was purchased from COSMO Bio Co. Ltd.

2.2 | Synthesis of TNT

TNTs were fabricated using an electrochemical anodization technique^{27–30} with a Ti sheet as the anode and a Pt sheet as the cathode. Commercially pure Ti sheets (2×1 cm) and Pt foil (2.5×2.5 cm) were cleaned in acetone, isopropyl alcohol, and methanol using ultrasonication for 15 min each. They were then sonicated in distilled ion-exchanged (DI) water for 5 min, rinsed with DI water, and dried. The Ti sheet was anodized using a two-electrode setup at room temperature and 60 V for 24 h with 100 mL of the electrolyte. Two types of TNT were prepared using different electrolytes. One was D-TNT from HF/DMSO, which was constituted of 2% of volume of 48% HF in DMSO, and another was E-TNT from HF/EG, which was constituted of 0.5% of mass of HF in EG. The voltage and anodization time were fixed in both the cases. The anode and cathode were separated by 2 cm in the electrolyte. After anodization, the TNT substrate was rinsed thrice with DI water and air-dried at room temperature.

The dried TNT film was annealed in an oxygen atmosphere at 540°C for 3 h at a heating rate of 1°C/min to obtain crystalline substrates. The TNTs prepared with HF/DMSO and HF/EG are denoted as D-TNTs and E-TNTs, respectively.

2.3 | Electrical polarization of TNT

Annealed TNT was polarized by placing the film between a pair of Pt-foil at 100 V of DC field and 400°C for 1 h.³¹ The polarization conditions were positively charged (P-polarized) from the cathode, negatively charged (N-polarized) from the anode, and as-prepared (non-polarized/0-polarized) TNT. To verify the reproducibility of the results, five samples were prepared for each condition.

2.4 | Characterization of TNT

The surface morphology of the TNT was observed using field-emission scanning electron microscopy (FE-SEM, S-4800, Hitachi Co.). The crystalline phases of the TNTs were identified by the powder X-ray diffractometry (XRD,

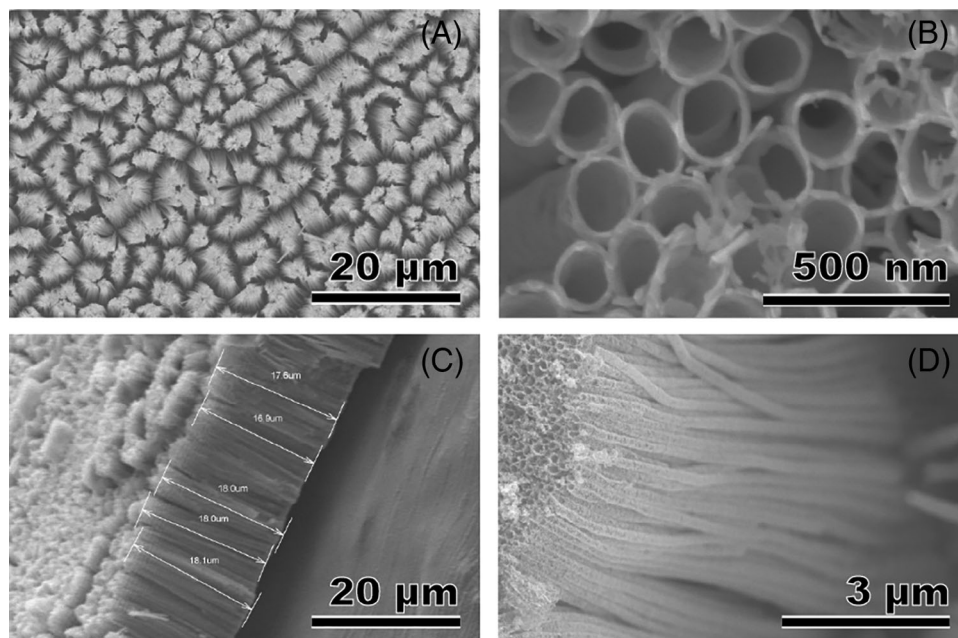


FIGURE 2 Field emission-scanning electron microscopy (SEM) images of D-TNTs. (A) Isle-like conjugated D-TNT, (B) top view (tube structure) of D-TNT, (C) thickness of D-TNT layer, and (D) side view of D-TNT (magnified [C] image). D-TNT, dimethyl sulfoxide; TNT, titania nanotubes.

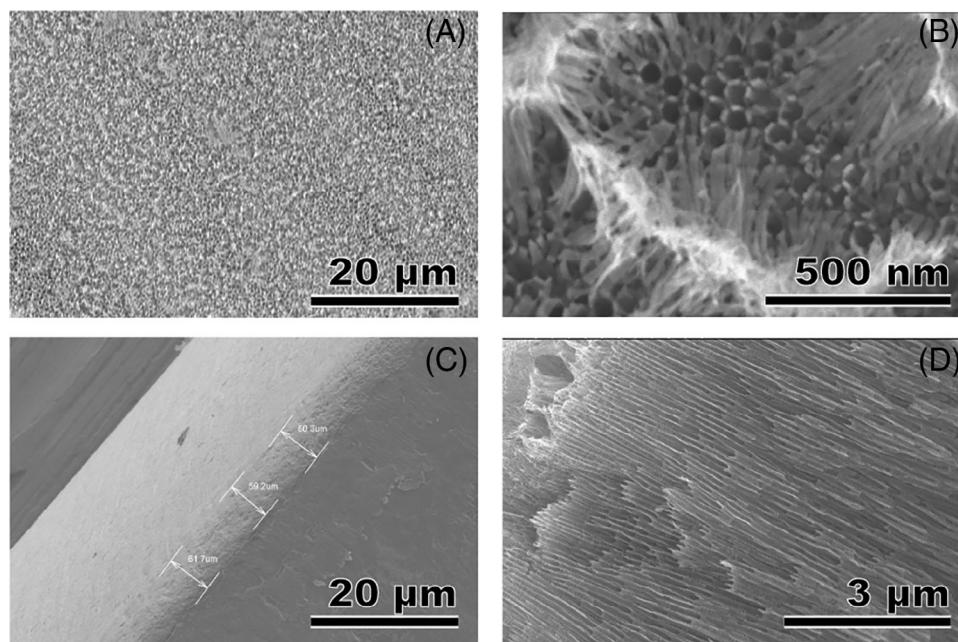


FIGURE 3 Field emission-scanning electron microscopy (SEM) images of E-TNTs. (A) Wall-like conjugated E-TNT, (B) top view (tube structure) of E-TNT shows that walls were thinner than D-TNT shown in Figure 2B, (C) thickness of E-TNT layer which was slightly thinner than that of D-TNT shown in Figure 2C, and (D) side view of D-TNT (magnified [C] image) which was denser than that of D-TNT shown in Figure 2D. E-TNT, ethylene glycol; D-TNT, dimethyl sulfoxide; TNT, titania nanotubes.

RINT-Ultima III, Rigaku Co.) from 10° to 80° of 2θ at a scanning rate of $2^\circ/\text{min}$ using carbon monochromatized $\text{CuK}\alpha$. The surface roughness of TNT was evaluated by the atomic force microscopy (AFM, E-Sweep with Nanonavi II, SII). The TNTs were qualitatively analyzed by energy-

dispersive X-ray spectroscopy (EDX, SU 8230, Bruker Inc.). To ensure that the TNT had a high electrical resistance and low electrical conductivity for electrical polarization, both were measured using a multimeter. The contact angle of the DI water on the TNT layer was measured using the ses-

sile water drop method and a goniometer (Contact Angle Meter DM-CE1, FAMAS, Kyowa) to evaluate its wettability.

2.5 | Antithrombogenicity evaluation

The thrombogenicity of the TNT was tested according to a previous report,³² using glass as a positive control and bare Ti as a control. The specimens were incubated in Ca- and Mg-free phosphate buffered saline at 37°C for 1 h. The cells were transferred to a six-well tissue culture plate with a pair of specimens in each well (Figure 1). A total of 1.5 mL of bovine blood was added to each well and was incubated at 37°C for 1 h. After the incubation, blood coagulation was activated by adding 150 µL of 0.1 M CaCl₂ aqueous solution in each well followed by mixing. Subsequently after 8–10 min of incubation, 5 mL of DI water was added to arrest coagulation. The specimens with thrombi were washed with PBS thrice, fixed with 37% formaldehyde for 1 h at room temperature, dehydrated serially using 60%, 70%, 80%, 90%, and 100% ethanol for each 15 min, and finally dried under vacuum. Digital images of samples and controls were captured using a digital camera (K-01, PEN-TAX, Japan) at 16.28 × 10⁶ pixels. The area of the thrombus formed on each sample in 1 × 1 cm from the edge of the Ti plate, as shown in Figure 1, is measured using ImageJ (Windows7, 64-bit Java 1.8.0_112, NIH).

2.6 | Statistical analysis

Statistical analysis was performed using one-way analysis of variance (ANOVA), followed by post hoc Tukey's analysis using Kaleida Graph (Ver. 4.5 (Macintosh)) to determine statistical significance among the samples at $p < 0.5$ as the level of significance.

3 | RESULTS AND DISCUSSION

3.1 | Surface characteristics of TNT

All the results shown in the following are for the annealed TNT, except for Figures 2 and 3 that show FE-SEM images of D- and E-TNTs, respectively. The D-TNT showed an isle-like structure formed by the conjugation of the D-TNT; in contrast, the E-TNT showed a wall-like structure. The diameters, wall thicknesses, and lengths of both TNT are summarized in Table 1. All D-TNT values were approximately two to three times larger than those of E-TNT. Furthermore, thinner fibrous nanotubes were observed on top of the E-TNT layer and appeared to form a denser coverage of the Ti surface. In contrast, the fluorine-

TABLE 1 Average diameter, wall thickness, and tube length of titania nanotubes (TNT).

| Sample | Diameter (nm) | Wall thickness (nm) | Tube length (µm) |
|--------|---------------|---------------------|------------------|
| D-TNT | 108.76 ± 2.55 | 30.39 ± 0.89 | 18.31 ± 1.93 |
| E-TNT | 53.83 ± 2.42 | 10.27 ± 1.07 | 11.01 ± 0.51 |

Abbreviations: E-TNT, ethylene glycol; D-TNT, dimethyl sulfoxide.

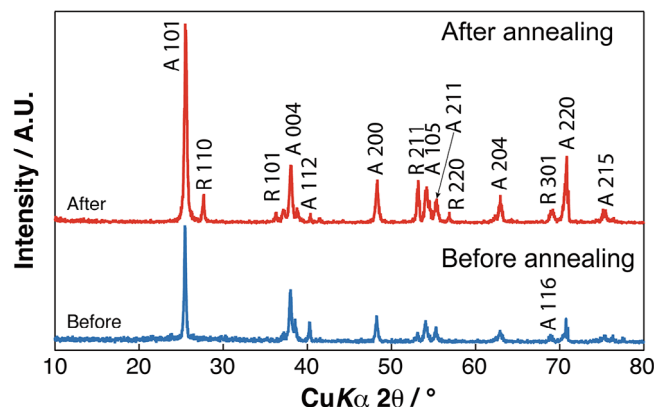


FIGURE 4 Powder X-ray diffractometry (XRD) patterns of D-TNT before and after annealing. Crystalline phases of D-TNT before annealing were anatase with small amount of rutile, but rutile phase was increased after annealing. D-TNT, dimethyl sulfoxide; TNT, titania nanotubes.

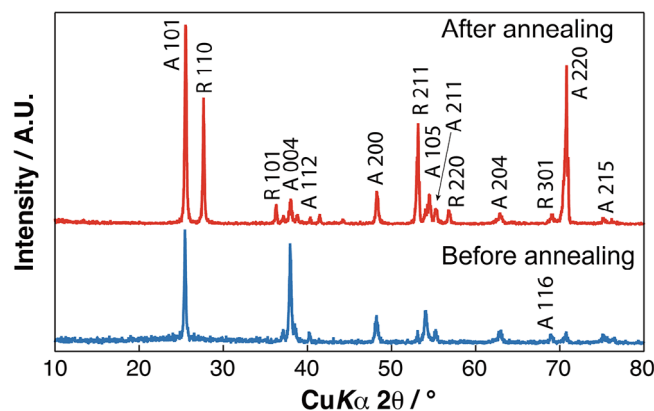


FIGURE 5 Powder X-ray diffractometry (XRD) patterns of E-TNT before and after annealing. Crystalline phases of E-TNT before annealing were anatase with small amount of rutile as the same as those of D-TNT. Increase of rutile phase after annealing was also found in D-TNT. E-TNT, ethylene glycol; D-TNT, dimethyl sulfoxide; TNT, titania nanotubes.

inhibiting nature of the HF/DMSO electrolyte aided in better control of the tubular morphology with pore diameters of 110 nm on the D-TNTs. As reported in the literature,^{33–35} the surface morphology was successfully controlled using the synthesis conditions. The EDX results showed that only Ti and oxygen were present in the TNT formed using both HF/DMSO and HF/EG, and no fluorine was detected.

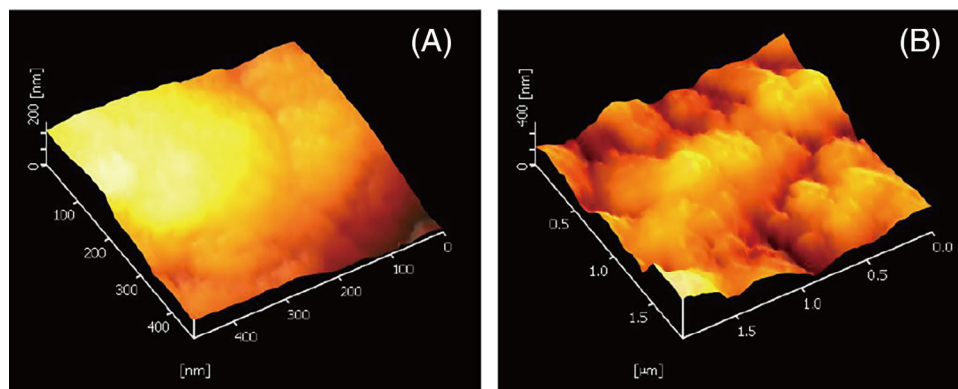


FIGURE 6 Atomic force microscopic images of (A) D-TNTs and (B) E-TNTs. Surface roughness of D-TNT shown in (A) were smoother than that of E-TNT (B). E-TNT, ethylene glycol; D-TNT, dimethyl sulfoxide.

TABLE 2 Electrical resistance and electrical conductivity values of Ti and titania nanotubes (TNT).

| Sample | Electrical resistance (Ω) | Electrical conductivity ($S \cdot m^{-1}$) |
|----------|------------------------------------|--|
| Titanium | 1.73×10^{-1} | 1.16×10^4 |
| D-TNT | 3.89×10^8 | 5.33×10^{-6} |
| E-TNT | 4.06×10^6 | 5.29×10^{-4} |

Abbreviations: E-TNT, ethylene glycol; D-TNT, dimethyl sulfoxide.

The powder XRD patterns of D- and E- TNT are shown in Figures 4 and 5, respectively. The crystalline phases of the TNT before and after annealing were anatase (A, JCPDS 21-1272) with a small amount of rutile (R, JCPDS 21-1276),^{36,37} the rutile phase increased after annealing in both TNTs owing to the higher stability of rutile than the anatase and brookite phases.

The surface roughness of the TNTs, characterized by AFM, is shown in Figure 6. The E-TNTs (Figure 6B) had greater roughness than the D-TNTs (Figure 6A). This could be due to the random layer-on-layer formation of TNT in the HF/EG electrolyte, which increased the surface roughness.

The electrical resistances of Ti and TNT are listed in Table 2, where TNT has a lower electrical conductivity than Ti. The maximum resistance of the TNT seems to be sufficient for electrical polarization. Figure 7 illustrates the results of the contact angle measurements before (0) and after polarization of the TNTs compared with bare Ti. No significant differences were observed for any surface, except for Bare Ti. TNT formation (0-D and 0-E) decreased surface contact angle drastically to 12%–15% of that of Bare Ti. Based on the contact angle (θ) of a water droplet on a surface, θ can be classified as superhydrophilic ($\theta \approx 0^\circ$), hydrophilic ($\theta < 90^\circ$), and hydrophobic ($\theta > 90^\circ$).³⁸ The contact angles of the 0-polarized TNTs

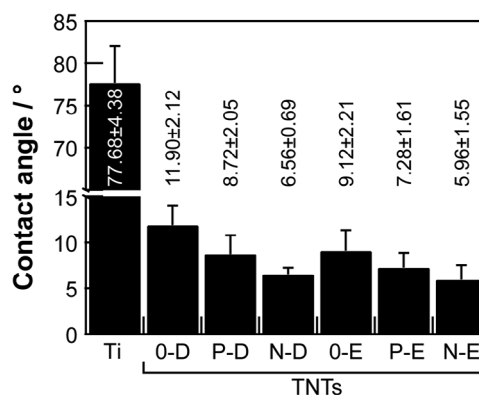


FIGURE 7 Water contact angle of bare Ti and titania nanotubes (TNTs). No significant differences were found between TNT surfaces.

were hydrophilic but not superhydrophilic, allowing antithrombogenic properties. From the contact angle point of view, polarized TNTs (P-D, N-D, P-E, and N-E) exhibited a trend of decreasing in their contact angles as seen in other polarized surface.³¹ These results indirectly demonstrated polarization of treated layers. Each N-polarized TNT showed a decreasing trend in the contact angle in comparison to each P-polarized TNT. However, contact angles of 6° – 9° are still not superhydrophilic like TiO_2 after UV irradiation and did not consider to be sufficient for antithrombogenic property as, similar to the 0-polarized TNTs, from the viewpoint of hydrophilicity.

3.2 | Antithrombogenicity

Typical results of the thrombus formation test are shown in Figure 8. The negative controls (glass and bare Ti) demonstrated huge thrombus formation. In contrast, thrombus formation on the TNTs was drastically suppressed. Non-

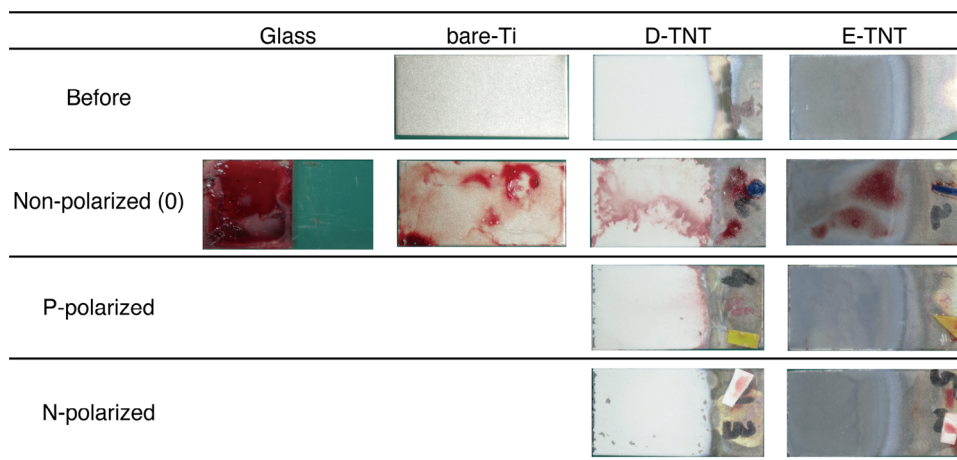


FIGURE 8 Typical thrombus formations on glass, bare Ti and titania nanotubes (TNTs). In comparison to negative controls, glass and bare Ti, thrombus formation on TNTs were suppressed drastically. Further, polarization of TNT drastically decreased thrombus formation.

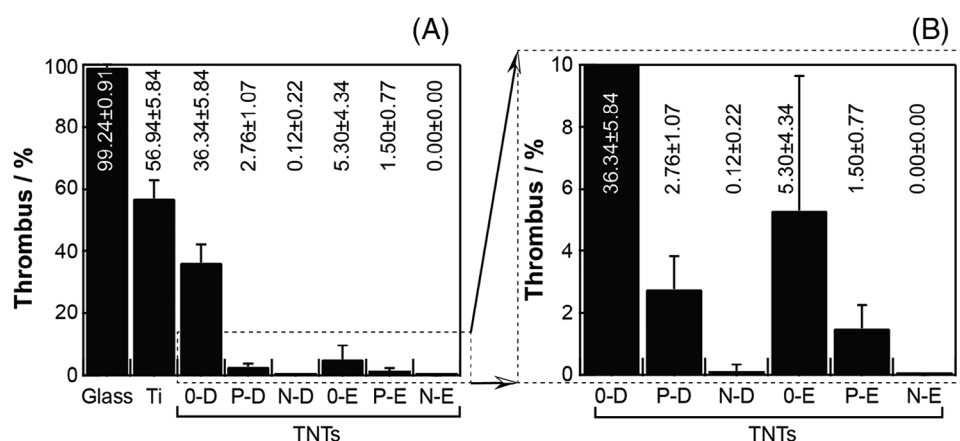


FIGURE 9 Relative thrombus coverage area, %, formed on glass, bare Ti and titania nanotubes (TNTs), (A) all results and (B) magnified results for TNTs. N-polarization of E-TNT completely inhibited thrombus formation.

polarized (0-polarized) TNTs still exhibited high thrombus formation; however, polarization drastically decreased thrombus formation. The image analysis results for thrombus formation are shown in Figure 9. One-way ANOVA revealed significant differences ($p < 0.00001$) between glass and other surfaces, bare Ti and TNTs, and non-polarized (0-polarized) D-TNTs and other TNTs. These results revealed that TNT formation should be effective for antithrombogenicity by both decreasing the contact angles and nanotopology to prevent adhesion of platelets and/or other proteins drastically (36.2% decrease) on the TNT. Enlargement of thrombosis results for TNTs shown in Figure 9B demonstrated a drastic decrease in thrombus formation on D-TNT at a rate of 92.4% by P-polarization and 99.7% by N-polarization, and that of 71.7% by P-polarization and 100% by N-polarization of E-TNT.

Positively charged P-polarized TNTs attract platelets electrostatically and are expected to form thrombi in comparison to non-polarized (0-polarized) TNTs; however, the surface charge and hydrophobicity of P-polarized TNTs could have a greater influence on inhibiting the attraction of other important proteins for coagulation, eventually leading to less thrombus formation when compared to that of 0-TNTs. The differences between D- and E-TNTs are considered to be due to differences in nanotopography, and smaller TNT could be better suited for the inhibition of thrombus formation. Negatively charged N-polarized TNTs showed little to no or quite small thrombus formation. In particular, the N-polarized E-TNTs exhibited no thrombus formation. Based on our in vitro results, we believe that negatively charged surfaces inhibit thrombus formation by exerting a repulsive force against negatively charged platelets, which is consistent with previous

studies.²⁶ TNTs have also been applied as drug reservoirs for antibiotics,³⁹ growth factors,⁴⁰ and antithrombogenic drugs. In addition, the high affinity of TiO₂ for cells is enhanced by polarization²⁴ and is a good substrate for vascular endothelial cell migration and formation of the vascular endothelium to prevent long-term thrombus formation. Therefore, E-TNT-TiO₂ is expected to be a good candidate for use in heart valves and other rigid devices in cardiovascular surgery.

4 | CONCLUSION

The Ti surface was fabricated using two types of TNTs, as per previous reports, and they were both positively and negatively polarized. The wettability increased because of polarization. The antithrombogenicities of polarized TNTs were drastically improved compared to those of non-polarized TNTs. Both nanotopographical properties and surface charges contribute to the inhibition of thrombus formation. Negatively polarized E-TNTs demonstrated no thrombus formation in the present experiments, which could be useful for rigid cardiovascular devices such as artificial heart valves.

ACKNOWLEDGMENTS

The authors are grateful to Profs. Akiko Nagai and Kimihiro Yamashita of Tokyo Medical and Dental University, Japan, for supporting the polarization of the TNTs. The authors would like to thank Editage (www.editage.jp) for English language editing.

CONFLICT OF INTEREST STATEMENT

The authors declare no conflict of interest.

ORCID

Masanori Kikuchi  <https://orcid.org/0000-0002-9451-8147>

REFERENCES

- Liu X, Yuan L, Li D, Chen G, Chen H, John LB, et al. Blood compatible materials: state of the art. *J Mater Chem*. 2014;B2:5718–38.
- Weber M, Steinle H, Golombek S, Hann L, Schlensak C, Wendel HP, et al. Blood-contacting biomaterials: in vitro evaluation of the hemocompatibility. *Front Bioeng Biotechnol*. 2018;6:99
- Jaffer IH, Weitz JI. The blood compatibility challenge. part 1: blood-contacting medical devices: the scope of the problem. *Acta Biomater*. 2019;94:2–10.
- Hisagi M, Nishimura T, Ono M, Gojo S, Nawata K, Kyo S. New pre-clotting method for fibrin glue in a non-sealed graft used in an LVAD: the KYO method. *J Artif Organs*. 2019;13:174–177.
- Lin W-C, Liu T-Yu, Yang M-C. Hemocompatibility of polyacrylonitrile dialysis membrane immobilized with chitosan and heparin conjugate. *Biomaterials*. 2004;25:1947–57.
- Chou C-C, Hsin S-W, Lin H-C, Yeh C-H, Wu R, Cherng W-J. Oxidized dopamine as the interlayer between heparin/collagen polyelectrolyte multilayers and titanium substrate: an investigation of the coating's adhesion and hemocompatibility. *Surf Coat Technol*. 2016;303:277–82.
- Weber N, Wendel HP, Ziemer G. Hemocompatibility of heparin-coated surfaces and the role of selective plasma protein adsorption. *Biomaterials*. 2002;23:429–39.
- Chou C-C, Zeng H-J, Yeh C-H. Blood compatibility and adhesion of collagen/heparin multilayers coated on two titanium surfaces by a layer-by-layer technique. *Thin Solid Films*. 2013;549:117–22.
- Jones JA. *Biomaterials and the foreign body reaction: surface chemistry dependent macrophage adhesion, fusion, apoptosis, and cytokine production*. Cleveland: Case Western Reserve University; 2007.
- Anderson JM, Rodriguez A, Chang DT. Foreign body reaction to biomaterials. *Semin Immunol*. 2008;20(2):86–100.
- Smith BS, Capellato P, Kelley S, Gonzalez-Juarrero M, Popat KC. Reduced in vitro immune response on titania nanotube arrays compared to titanium surface. *Biomater Sci*. 2013;1:322–32.
- Smith BS, Yoriya S, Johnson T, Popat KC. Dermal fibroblast and epidermal keratinocyte functionality on titania nanotube arrays. *Acta Biomater*. 2011;7:2686–96.
- Smith BS, Yoriya S, Grissom L, Grimes CA, Popat KC. Hemocompatibility of titania nanotube arrays. *J Biomed Mater Res A*. 2010;95A(2):350–60.
- Brunetti V, Maiorano G, Rizzello L, Sorce B, Sabella S, Cingolani R, et al. Neurons sense nanoscale roughness with nanometer sensitivity. *Proc Natl Acad Sci USA*. 2010;107(14):6264–69.
- Buttiglieri S, Pasqui D, Migliori M, Johnstone H, Affrossman S, Sereni L, et al. Endothelization and adherence of leucocytes to nanostructured surfaces. *Biomaterials*. 2003;24(16):2731–38.
- Peng L, Eltgroth ML, Latempa TJ, Grimes CA, Desai TA. The effect of TiO₂ nanotubes on endothelial function and smooth muscle proliferation. *Biomaterials*. 2009;30(7):1268–72.
- Junkar I, Kulkarni M, Benčina M, Kovač J, Mrak-Poljšak K, Lakota K, et al. Titanium dioxide nanotube arrays for cardiovascular stent applications. *ACS Omega*. 2020;5(13):7280–89.
- Tsai C-C, Chang Y, Sung H-W, Hsu J-C, Chen C-N. Effects of heparin immobilization on the surface characteristics of a biological tissue fixed with a naturally occurring crosslinking agent (genipin): an in vitro study. *Biomaterials*. 2001;22:523–33.
- Campoccia D. In vitro behaviour of bone marrow-derived mesenchymal cells cultured on fluorohydroxyapatite-coated substrata with different roughness. *Biomaterials*. 2003;24:587–96.
- Cai K, Yao K, Cui Y, Yang Z, Li X, Xie H, et al. Influence of different surface modification treatments on poly (D,L-lactic acid) with silk fibroin and their effects on the culture of osteoblast in vitro. *Biomaterials*. 2002;23:1603–11.
- Sun L, Li Y, Liu X, Jin M, Zhang L, Du Z, et al. Cytotoxicity and mitochondrial damage caused by silica nanoparticles. *Toxicol In Vitro*. 2011;25:1619–29.
- Braydich-Stolle LK, Schaeublin NM, Murdock RC, Jiang J, Biswas P, Schlager JJ, et al. Crystal structure mediates mode of cell death in TiO₂ nanotoxicity. *J Nanopart Res*. 2009;11:1361–74.

23. Sabino RM, Kauk K, Madruga LYC, Kipper MJ, Martins AF, Popat KC. Enhanced hemocompatibility and antibacterial activity on titania nanotubes with tanfloc/heparin polyelectrolyte multilayers. *J Biomed Mater Res A*. 2020;108(4):992–1005.
24. Chen X, Mao SS. Titanium dioxide nanomaterials: synthesis, properties, modifications, and applications. *Chem Rev*. 2007;107(7):2891–959.
25. Bartlet K, Movafaghi S, Kota A, Popat KC Superhemophobic titania nanotube array surfaces for blood contacting medical devices. *RSC Adv*. 2017;7:35466–76.
26. Saito H, Murabayashi S, Mitamura Y, Taguchi T. Unusual cell adhesion and antithrombogenic behavior of citric acid-cross-linked collagen matrices. *Biomacromolecules*. 2007;8:1992–98.
27. Sabino RM, Kauk K, Movafaghi S, Kota A, Popat KC. Interaction of blood plasma proteins with superhemophobic titania nanotube surfaces. *Nanomed Nanotech Biol Med*. 2019;21:102046.
28. Mor GK, Varghese OK, Paulose M, Shankar K, Grimes CA. A review on highly ordered, vertically oriented TiO₂ nanotube arrays: fabrication, material properties, and solar energy applications. *Sol Energy Mater Sol Cells*. 2006;90(14):2011–75.
29. Roy P, Berger S, Schmuki P. TiO₂ nanotubes: synthesis and applications. *Angew Chem Int Ed Engl*. 2011;50(13):2904–39.
30. Ruan C, Paulose M, Varghese OK, Mor GK, Grimes CA. Fabrication of highly ordered TiO₂ nanotube arrays using an organic electrolyte. *J Phys Chem B*. 2005;109(33):15754–59.
31. Sheng J, Fukami T, Karasawa J. X-ray photoemission spectroscopy (XPS) and thermally stimulated current (TSC) studies on the resistance degradation of iron-doped titania ceramics. *J Am Ceram Soc*. 1998;81:260–62.
32. Song Y-Y, Schmidt-Stein F, Bauer S, Schmuki P Amphiphilic TiO₂ nanotube arrays: an actively controllable drug delivery system. *J Am Chem Soc*. 2009;131(12):4230–32.
33. Ma C, Nagai A, Yamazaki Y, Toyama T, Tsutsumi Y, Hanawa T, et al. Electrically polarized micro-arc oxidized TiO₂ coatings with enhanced surface hydrophilicity. *Acta Biomater*. 2012;8:860–65.
34. Neupane MP, Park ILS, Bae TS, Yi HoK, Watari F, Lee MHo, Synthesis and morphology of TiO₂ nanotubes by anodic oxidation using surfactant based fluorinated electrolyte. *J Electrochem Soc*. 2011;158(8):C242–45.
35. Zhang S, Li Y, Xu P, Liang K. Effect of anodization parameters on the surface morphology and photoelectrochemical properties of TiO₂ nanotubes. *Int J Electrochem Sci*. 2017;12:10714–10725.
36. Joseph S, David TM, Ramesh C, Sagayaraja P. The role of electrolyte pH in enhancing the surface morphology of TiO₂ nanotube arrays grown on Ti substrate. *Int J Sci Eng Res*. 2014;5(3):85–91.
37. Kang I-K, Kwon OH, Kim MK, Lee YM, Sung YK. In vitro blood compatibility of functional group-grafted and heparin-immobilized polyurethanes prepared by plasma glow discharge. *Biomaterials*. 1997;18(16):1099–107.
38. Kota AK, Kwon G, Tuteja A. The design and applications of superomniphobic surfaces. *NPG Asia Mater*. 2014;6:e109. <https://doi.org/10.1038/am.2014.34>
39. Popat KC, Eltgroth M, Latempa TJ, Grimes CA, Desai TA. Decreased *Staphylococcus epidermis* adhesion and increased osteoblast functionality on antibiotic-loaded titania nanotubes. *Biomaterials*. 2007;28(32):4880–88.
40. Popat KC, Eltgroth M, Latempa TJ, Grimes CA, Desai TA Titania nanotubes: a novel platform for drug-eluting coatings for medical implants? *Small*. 2007;3(11):1878–81.

How to cite this article: Muralidhar JR, Sakthivel K, Sridharan M, Kikuchi M. Influence of electrical polarization on thrombogenicity of titania nanotubes. *Int J Ceramic Eng Sci*. 2024;e10214. <https://doi.org/10.1002/ces2.10214>